MULTIAXIAL FATIGUE: A BRIEF REVIEW

K. J. Miller and M. W. Brown

Department of Mechanical Engineering, University of Sheffield, Mappin Street, Sheffield S1 3JD, England

ABSTRACT

A brief review of recent developments in fatigue failure studies under mixed mode loading, in terms both of the externally applied forces and the manner of crack growth, is presented.

Classical approaches to multiaxial fatigue correlations are shown to be inadequate and new theories are presented in terms of crack growth mechanics and three dimensional deformation behaviour that relate the failure process to specific crack growth stages, the orientation of crack growth planes, fracture modes and crack growth rates.

The paper discusses multiaxial fatigue by specifically considering test facilities, specimen geometry, anisotropy, cumulative damage, out-of-phase loading, cyclic deformation behaviour, mixed mode cracking and life assessment techniques.

Finally a bibliography of recent work on multiaxial fatigue studies at Sheffield is presented to permit those interested in this relatively new subject to have access to a wider range of literature.

KEYWORDS

Biaxial and multiaxial fatigue; biaxial crack propagation; life assessment; out-of-phase cyclic loading; mixed-mode cracking; cumulative damage; anisotropy.

INTRODUCTION

The failure by fatigue of engineering components and structures places a heavy economic loss, as well as a danger to life, on the peoples of many countries. And yet after more than one hundred years of research we are still far from solving the varied problems associated with fracture caused by the cyclic application of forces on engineering artefacts when these are

placed in their working environment. This is due to their complex geometrical shape, the various methods and techniques by which they are produced, the nature of the environment in which they are placed, and the cyclic stress-strain state to which they are subjected. Furthermore under the random loading conditions observed in service it is sometimes difficult to define a cycle which contributes to the accumulation of fatigue damage.

Recent developments in complex fatigue research, particularly under multi-axial and mixed-mode fracture conditions, have clarified rather than complicated our understanding of the processes that cause fracture, and have revealed new aspects of the problem which indicate that we have been delayed in our progress towards solutions by several misconceptions. In order to make further progress towards solutions it is important to recognise these misconceptions and then to concentrate on those issues that have a significant impact on the creation and accumulation of fatigue damage.

This paper does not intend to review the history of fatigue but it is thought necessary to briefly outline some serious misconceptions and indicate why they are wrong not only to help the design engineer to avoid costly mistakes, but also to focus the attention of the research worker on the factors that influence fatigue failure. In these respects knowledge of how multiaxial stress and strain fields influence crack initiation and propagation is of paramount importance since most laboratory research involves tests on simple-geometry specimens subjected only to either axial, torsional or bending forces. Seldom are such forces applied in combination in the laboratory. However, in the real world complex cyclic forces of a continuously varying nature may be imposed over a wide range of conditions. One such example that is most pertinent to this sub-continent is the railway line of which there are many thousands of miles. The plane of a typical fatigue fracture in a railway line is subjected to continuously varying shear loading and bending stress, but since these are not in-phase with one another, the rail is subjected to a rotating stress field. A more complex problem is that of thermal stress transients induced into the surfaces of a gas turbine blade and which create a biaxial stress field. Both of these examples necessitate a new outlook to questions such as (i) how is fatigue damage created, (ii) how does it accumulate and (iii) at what rate does it accumulate. These questions can only be answered in relation to the more general multiaxial stress situation if the term "damage" can be quantified. The present paper suggests that damage should be equated to crack length and the rate of damage accumulation is therefore given by the rate of crack growth. Hence it is important to relate the crack to the three-dimensional stress field in which it is situated. This is the first step in any multiaxial fatigue study.

Figure 1(a) represents the actual stress state to which a structure is subjected whilst Fig. 1(b) represents a simulation test carried out on a specimen in a laboratory in order to determine the probable response of the structure. The simulation is complete in that it reproduces the same environment, temperature conditions, material composition, processing route and final heat treatment, as well as an identical stress-strain state. It may therefore be argued from classical fatigue theories that since both the specimen and the structure have an identical equivalent stress-strain state they will fail by fatigue at the same instant. However, this is not so. The structure may fail in as few as 10,000 cycles of loading and the laboratory specimen may never fail, should the former have a microscopic defect such as a crack of a length equal to about a grain diameter and which is perpendicular to the $\Delta\sigma_1$ direction, while in the laboratory sample this

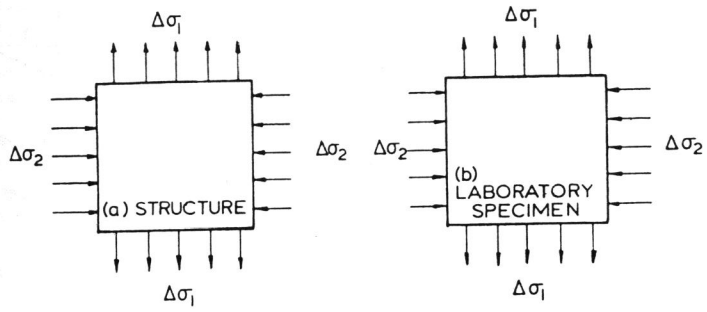

Fig. 1 Identical biaxial stress-strain states of a laboratory specimen and the critical part of a structure.

minute undetected microscopic defect is perpendicular to $\Delta\sigma_2$. This simple example explains one major misconception; the reason why a single parameter such as an equivalent stress or strain approach (e.g. a Von Mises criterion) can not correlate all fatigue test data. It also indicates the necessity to appreciate the orientation of a defect, not only with respect to the stress-strain state but also with the surface plane.

This paper presents a brief review of the relationships between three-dimensional cyclic strain fields and the type, shape, orientation, mode, growth rate and instability of fatigue cracks.

FRACTURE BEHAVIOUR

Fatigue failure is due to fracture processes and, as explained above, it is difficult to relate deformation parameters to the conditions that cause a crack to grow. No acceptable theory yet exists that relates the cessation of elastic behaviour, i.e. yield stress, to the strain that causes gross instability in a ductile metal, and so it is not surprising that the classical yield theories do not have universal applicability to fatigue failure.

The reason is relatively simple. Two parameters, not one, have a marked influence on the failure process. In general terms one parameter controls the orientation of the defect that leads to failure while its magnitude determines the growth rate of the defect. The second parameter modifies the growth rate. In fatigue the two parameters are best described with the aid of Fig. 2. When a load is applied that deforms a material, the resulting three-dimensional change in shape may be described by the three Mohr's circles of strain of Fig. 2(a), all of which decay on release of the load. The important cyclic variation therefore is the size of the largest circle which is the maximum shear strain γ; this equals $(\varepsilon_1-\varepsilon_3)$. The second important parameter is the position of this circle in strain space which equals $0.5\ (\varepsilon_1+\varepsilon_3)$. The first parameter controls the deformation of the body via shear processes on slip planes. The second parameter, ε_n, is the

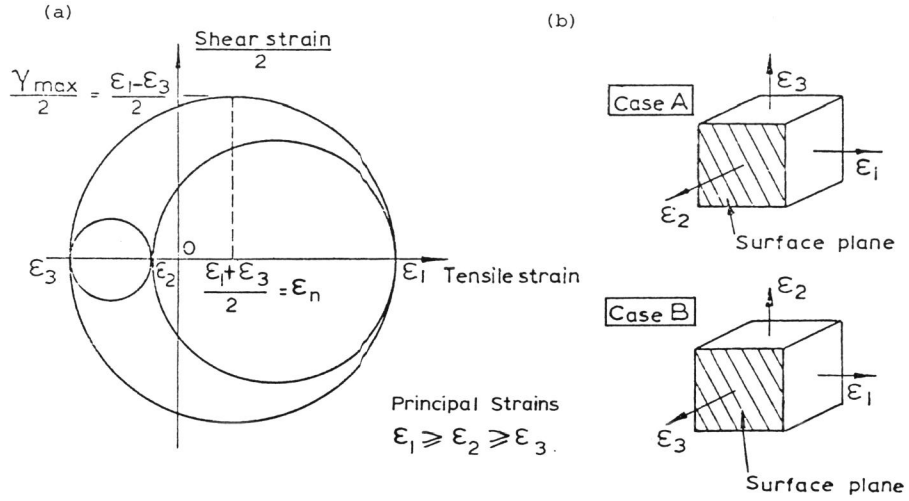

Fig. 2 Mohr's Circles of Strain and the two cases of strain state orientation with respect to a free surface.

normal strain across the slip plane. The importance of each of these parameters on fracture processes will become more obvious in latter sections.

In Fig. 2(b) the orientation of the three principal strains is shown with respect to the surface plane. It is clear that only these two cases are admissible. For Case A the intermediate principal strain is normal to the free surface, while for Case B the orientation of ε_2 is such that it is parallel to the surface. Since fatigue cracks invariably start from a free surface it is important to realise that by considering the three dimensional strain state in relation to the orientation of the surface, two quite distinct crack systems can be generated. These are now described.

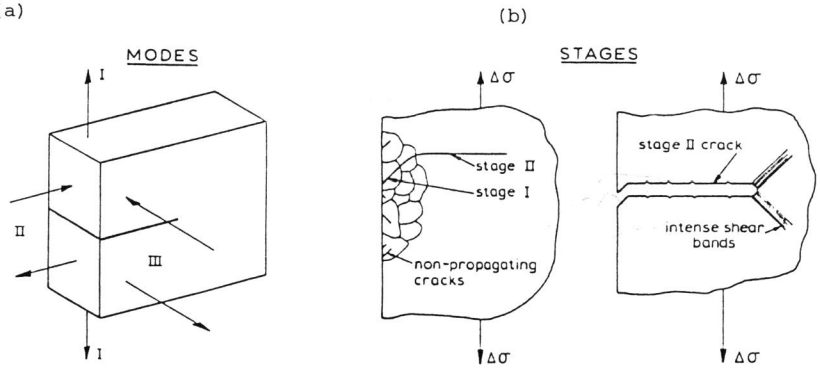

Fig. 3 Modes and Stages of fatigue crack growth

Cracks extend by the application of forces that may be resolved into three directions that cause pure mode I, pure mode II, or pure mode III growth, see Fig. 3(a). Usually cracks grow by a mixture of these three different modes. However, unless the material is highly anisotropic (see pages 22&23) all fatigue cracks can be classified into a much simpler system of stage I and stage II crack growth (1), see Fig. 3(b). Stage I cracks grow along planes of maximum shear and, even in push-pull axial tests (especially close to the fatigue limit), their phase of growth can dominate the lifetime period. Stage II cracks also extend in ductile materials by a process of decohesion on two equally intense, shear planes which the cracks bisect, and hence grow in a direction that is perpendicular to the direction of maximum tensile stress. Note however that the driving mechanism is still due to a shearing process.

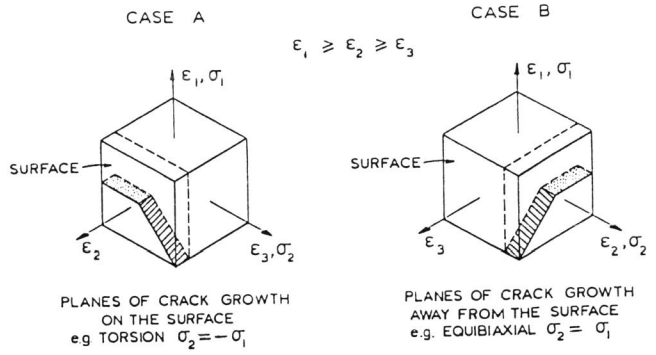

Fig. 4 State I and Stage II crack growth planes for Case A and Case B strain states

Figure 4 shows how Stage I and Stage II cracks grow in relation to the surface for both Case A and Case B three dimensional strain states (2). The Case A, Stage I growth plane is shown shaded while the Case A Stage II growth plane is dotted. The important point here is that the Case A cracks are contained in the surface layers. This state occurs in torsion testing and the growth of these cracks is by mode II along the surface and mode III in depth. For Case B the situation is far more dangerous with the cracks growing away from the surface; again the Stage I crack and the Stage II crack are shown dashed and dotted respectively. The Stage I crack is initially driven inwards by a mode II mechanism but mode I plays an increasing role until finally the Stage II crack is dominated by a mode I opening mechanism.

MULTIAXIAL FATIGUE TEST SPECIMENS

The shape and size of specimens is of crucial importance in multiaxial fatigue testing. From previous sections it is obvious that it is necessary to control and accurately measure the exact three-dimensional (3-D) stress-strain state and maintain the condition throughout each individual test. Note that in cumulative damage tests (see pages 20-22) it is required to periodically re-orientate the 3-D field with respect to both the surface and the initial crack planes. One important additional feature of 3-D tests

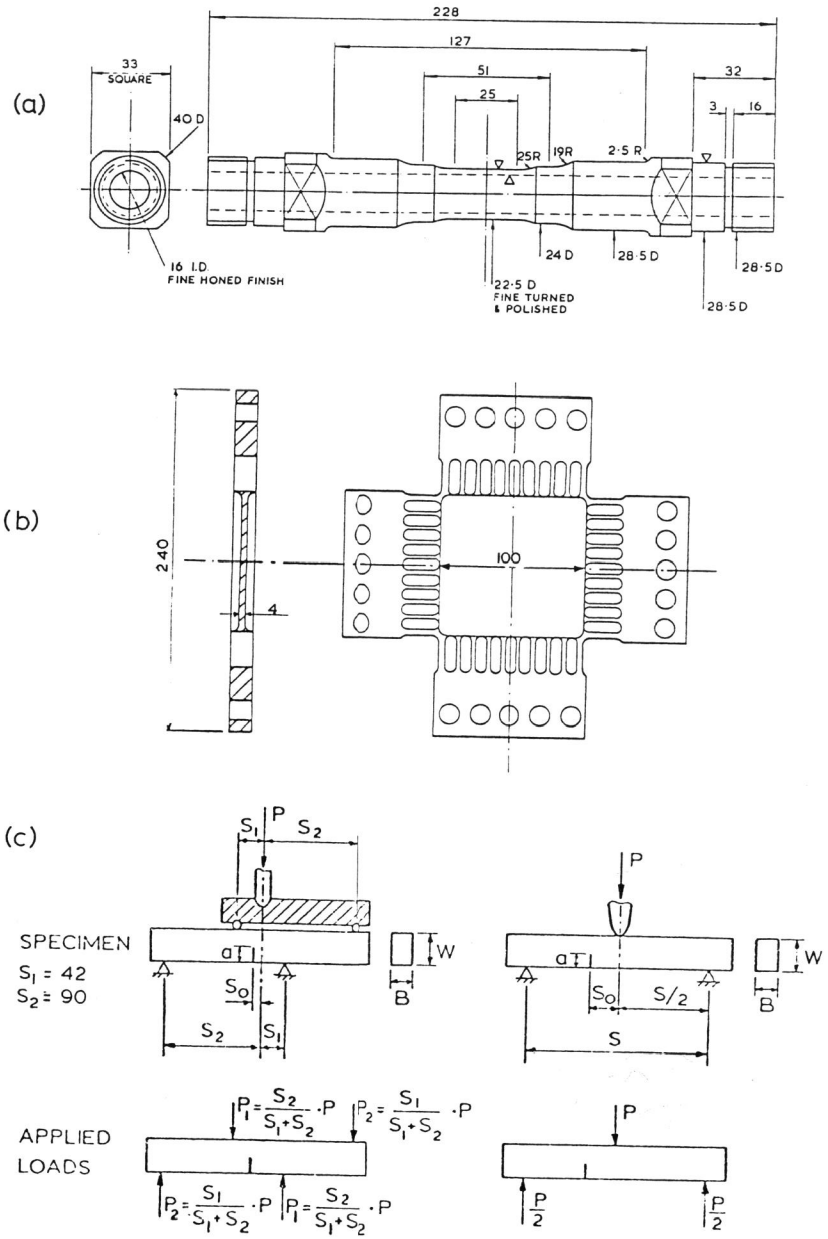

Fig. 5 Types of Specimen used in multiaxial fatigue studies (all dimensions in mm)

is the requirement of monitoring cracks, particularly their growth direction and speed.

These requirements mean that specimens are expensive to produce and Fig. 5 gives some examples of the types of specimen we use at Sheffield. The tubular test piece is one used for both low-cycle, high-strain fatigue tests and for studies of multiaxial fatigue plus creep (and dynamic ageing) interactions at high temperatures. In uniaxial tests cracks sometimes propagate from honing marks in the bore although other cracks are also observed on the polished outer surface. With the addition of a torsional strain however, the stress gradient across the wall thickness excludes the possibility of failure initiating from the bore and multiple cracking is observed over the outer gauge section.

Although an exact stress-strain analysis of plastically deformed tubes subjected to cyclic torsion is now available (3), an internal to external diameter ratio of the tube of $\sim$0.7 was chosen to permit an approximation to thin walled tube analysis for complex out-of-phase loading conditions, while at the same time providing sufficient stiffness to achieve fatigue lives as low as 100 cycles without causing buckling.

The cruciform test specimen shown in Fig. 5 was specifically designed to investigate Case B type cracks subjected to various biaxial stress states usually in the range $-1 \leqslant \Lambda \leqslant +1$, where $\Lambda = \sigma_2/\sigma_1$ (see Fig. 1). Starter cracks are placed in the centre of the specimen with the aid of a spark-erosion machine. The slots on each loading arm permit a uniformly distributed load to be applied at each edge while at the same time allowing sufficient lateral flexibility to accommodate the strain imposed by the other mutually perpendicular arms. A uniform strain distribution is maintained over almost the whole of the 100 mm square centre gauge section thereby permitting a wide range of crack lengths and crack angles to be studied. Due to the additional thickness at the fillet radius which provides an edge constraint, the equivalent width W* of this specimen for the determination of stress intensity values is increased by only 1.9 mm, i.e. W* = 101.9 mm. These specimens are even more expensive than the tubular specimens and have to be produced on NC end-mill machines. The centre section is finally highly polished to facilitate optical crack growth measurements.

The cheapest form of specimen is the rectangular section bend specimen, also shown in Fig. 5. Analysis of the bending moment and shear force diagrams for both the four point and three point bend configurations shows that by a judicial positioning of the crack in relation to the points of application of forces, it is possible to cover the whole range of crack growth modes from pure mode I through pure mode II. Adaption of this testing rig at Sheffield will also permit additional interactive effects due to mode III loading to be investigated so that the behaviour of cracks in components and structures subjected to axial, bending and torsional forces can be determined. Of particular interest in these studies is the determination of conditions for the change-over of crack growth mode and checking of crack growth theories for mixed mode loading conditions.

In conclusion it should be stated that the tubular specimens have been predominantly used for high strain studies; the cruciform specimens may be used for bulk stress conditions up to and just beyond yield; and the three point and the four point bend Linear Elastic Fracture Mechanics (LEFM) type specimens are for bulk stress levels less than a quarter of yield stress of

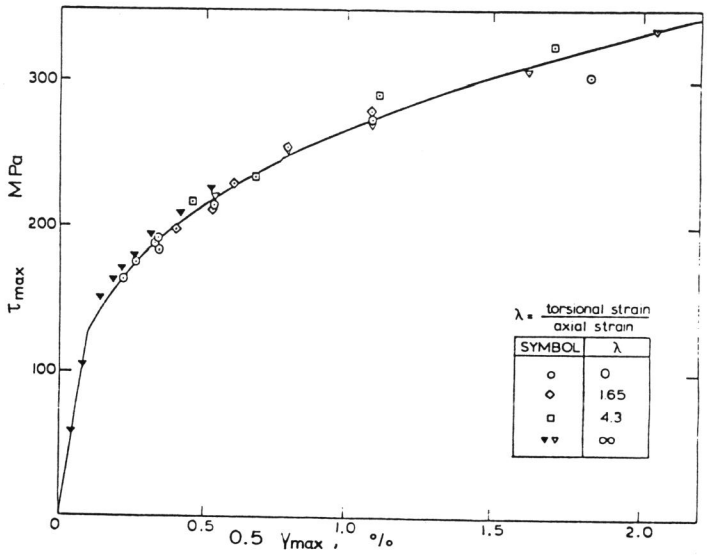

Fig. 7 The cyclic stress-strain curve for AISI 316 stainless steel at 400°C

theory (10). A typical result in shown in Fig. 7 for four different λ ratios. In Fig. 7 the solid points are from a multiple step test while the open points are for the stress amplitude values in strain range controlled tests, taken at half fatigue life. All points were obtained from tests in which the torsional and axial strain ranges were in-phase with each other. Under out-of-phase loading, the rotation of the principal axes causes an apparent distortion of the hysteresis loops and the traditional definitions of the elastic or plastic strain range components of the total-strain range are more difficult to ascertain. Nevertheless by determining the maximum shear strain amplitude operative within a cycle, and its corresponding shear stress, a cyclic stress-strain curve for in- and out-of-phase conditions can be obtained (see Fig. 8). The correction factor, F, is a measure of the effect of rotation of the principal axes which causes additional work-hardening for the reasons mentioned previously.

Crack Planes and Crack Shapes

Figure 9 shows examples of stage I and stage II crack orientation for specific examples of strain states. It should be noted that, because of the possibility of crack initiation occurring simultaneously in several grains, all with different inclinations, the fracture surface can exhibit a few ridges , where the early stage I cracks have linked up. Examination of some 69 multiaxial in-phase, low-cycle fatigue specimens after fracture under various conditions of strain state, strain rate and temperature permitted an evaluation of crack orientation from the multiple cracks found on the large area of uniform strain in the gauge length of a tubular specimen. These results are given in Fig. 10. In this figure Ω is the inclination of the crack to the specimen axis and the strain state is given

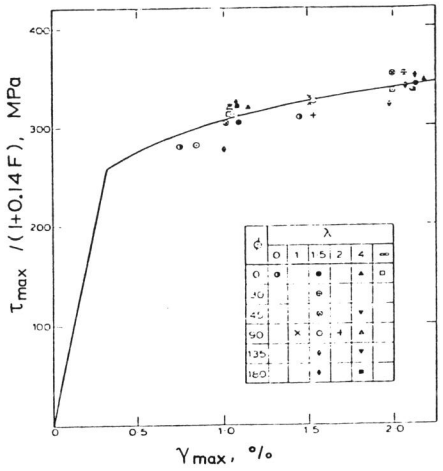

Fig. 8 The out-of-phase, biaxial cyclic stress-strain curve of a 1% Cr-Mo-V steel

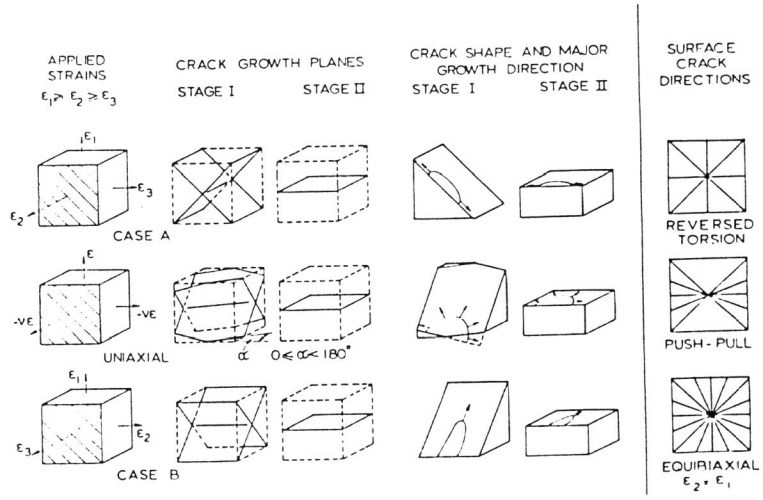

Fig. 9 Crack plane orientations and crack shapes for different states of strain

by the function

$$\psi = 0.5 \tan^{-1}\left[\frac{2\lambda}{3}\right] \qquad [4]$$

where λ is the ratio of the applied torsional and axial strains. It is clear

that all but one system of cracks are either stage I or stage II, the one exception being probably due to previously observed anisotropy (see later discussion). It should also be noted that some specimens exhibited all the three possible sets of crack orientations shown in Fig. 10.

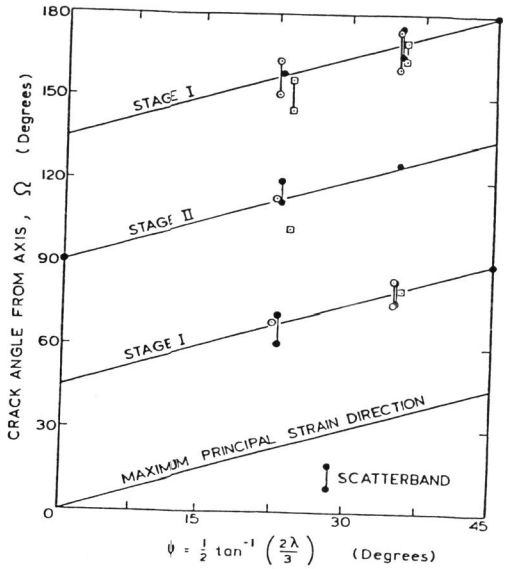

Fig. 10 Inclination of cracks for various strain states ○ 1% Cr-Mo-V steel (20°C), ● 1% Cr-Mo-V steel (565°C) □ AISI 316 stainless steel (400°C)

One set of interesting observations at 565°C in 1% Cr-Mo-V steel involved the transition from stage II cracks, initiated in the presumably brittle oxide surface film, to stage I crack growth on reaching a certain depth. This effect was more pronounced at lower strain rates and a detailed examination (11) of the transition of stage I to stage II cracks, and vice-versa, indicated its dependence on the applied strain state.

Finally, Fig. 9 shows how the applied strain state influences the development of crack shape. Case A type cracks found in torsion fatigue studies propagate along the surface by mode II and into the interior by mode III. The cracks during the major part of lifetime are shallow and not detrimental to the load-carrying capacity of the structure. Case B cracks, however, penetrate relatively rapidly into the bulk and the length of the major axis of the elliptical crack shape, in a direction away from the free surface, increases as ε_n decreases. The way that the shape of the cracks is determined by the multiaxial strain state is now of major importance in many structures such as offshore structures and gas pipelines, since here large cracks can develop in comparison to the plate thickness and the multi-axial strain state may vary substantially around the crack profile causing variations in shape and hence lifetime.

CRACK PROPAGATION RATES

If a two-parameter description is necessary to characterize fatigue endurance, it follows that crack propagation must also require a two-parameter description for correlating different stress-strain states.

To emphasise this point Fig. 11 describes the effect of the second parameter ε_n on fatigue lifetime with the first parameter $\Delta\gamma$ constant at 3%. It follows that multiaxial fatigue tests can also be carried out keeping either the maximum octahedral shear strain (or stress) or the maximum tensile stress constant, but by changing another parameter that helps describe stress or strain space, fatigue lives will correspondingly change. This important consideration is effectively hidden when analysing push-pull data, because the magnitude of ε_n is always $\gamma/6$ (assuming constancy of volume) and its orientation never changes in relation to the direction of the applied tensile load. Figure 11 shows that with increasing ε_n, which effectively assists the crack opening displacement and hence crack growth, endurance decreases and this effect is true for all the strain states studied. This research (12) showed that cracks always initiated on planes of maximum shear under all loading conditions. For the special case of the out-of-phase angle $\phi = 90°$ and $\lambda = 1.5$ the shear strain range is identical on all planes and cracks tend to grow in all directions. The crack system that dominated and eventually caused failure was that which suffered the maximum value of ε_n. This fact and data such as that illustrated in Fig. 11 confirm the necessity to have a two parameter description of the strain state to describe fatigue crack propagation under any 3-D strain state including the special case of uniaxial loading.

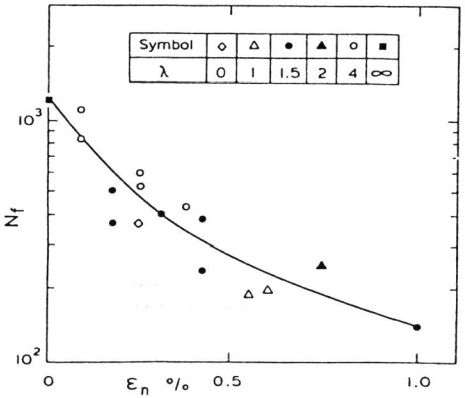

Fig. 11 The effect on endurance of ε_n keeping the shear strain range constant

The growth rate of fatigue cracks is usually presented in the literature by plots of da/dN against ΔK, the range of stress intensity factor; as indeed are many papers in this conference. This factor is determined from considerations of the elastic stress-strain field in the vicinity of the crack-tip. However Linear Elastic Fracture Mechanics (LEFM) does not take account of

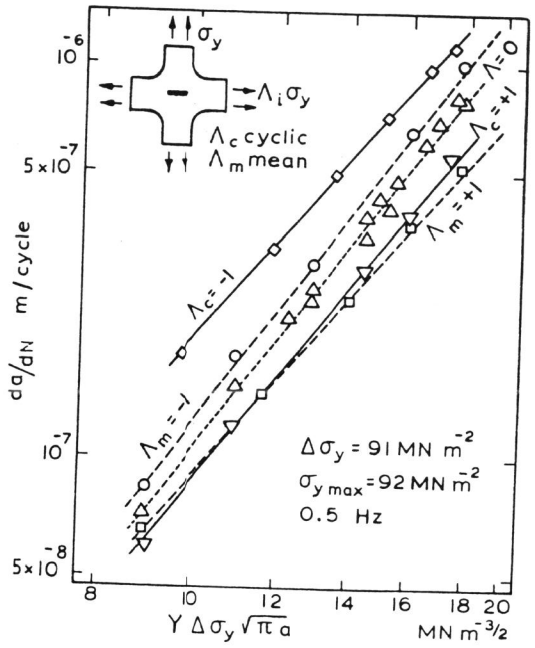

Fig. 12 The effect of stress biaxiality on crack propagation rates in RR58 aluminium alloy

anisotropy or plasticity, nor the stress which is perpendicular both to the crack front and the stress that is normal to the crack plane; this stress has no effect on the LEFM crack tip singularity condition. However it has been shown (13) that crack tip plasticity conditions are affected by this stress and hence such stresses should affect crack growth rates. Experiments have shown this to be so (14), with the maximum effect being noted under shear loading conditions; see Fig. 12 which applies to stage II, mode I type cracks. The equation describing the data of Fig. 12 are of the form

$$da/dN = A\,(\Delta K)^m \qquad [5]$$

where $\Delta K = Y\Delta\sigma_y\sqrt{\pi a}$

and A is stress state dependent, i.e. the curves show that a compressive non-singular stress, either of a static or cyclic nature, accelerates growth, while tensile stresses decrease it in this RR58 aluminium alloy. The same result has been found for 6061-T4 and T6 (15) and 6061-T651 aluminium alloy (16) PVC (17), mild steel (18) and to a small extent in L70 aluminium alloy (19). Those materials that do not exhibit this biaxiality effect are those of very limited ductility, i.e. those materials that suffer negligible crack tip plasticity prior to fast fracture.

LIFE ASSESSMENT

The effect of stress biaxiality is illustrated in Fig. 13 which shows that the low stress level results given in Fig. 12 require a two-parameter description. The major fracture parameter is $Y\Delta\tau\sqrt{\pi a}$, but a second parameter such as $Y\Delta\sigma_n\sqrt{\pi a}$ is necessary to account for different stress ratios. It is now possible to predict the form of the life contour curves on the Γ plane for this RR58 alloy in the low-cycle, high-strain fatigue regime. In deriving the curves of Fig. 14, a Tresca flow rule was used to determine the biaxial cyclic stress-strain curve so that the stress intensity factor ΔK, of equation [5] could be replaced by a strain intensity factor, i.e. $\Delta\gamma\sqrt{\pi a}$, which ought to be more suitable for low-cycle fatigue conditions. The new strain based equation is integrated between initial and final crack lengths of 15 μm (surface finish) and one tenth of the wall thickness respectively. The biaxial effect is governed only by the term A in equation [5]; whose values are taken from Fig. 12 in which m = 3.377. Empirical data from Ellison and Andrews (20) for RR58 are also shown in this figure, which is fitted to the equation

$$0.5\gamma/g + \varepsilon_n/h = 1 \qquad [6]$$

for case A loading. It can be seen that the crack growth equation for RR58 predicts the fatigue life very well for low-endurance, high-strain fatigue. Here the Tresca correlation for the Case B cracking system gives a reasonable and safe estimate of fatigue strength.

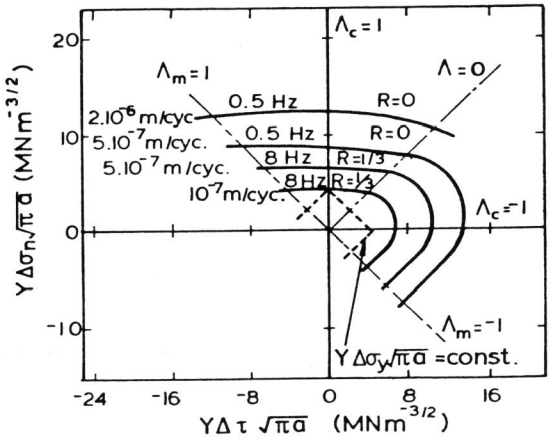

Fig. 13 Contours of fatigue crack growth rates for RR58 aluminium alloy; the dotted line is the LEFM prediction

To conclude this section a modification to the Coffin-Manson equation, Eqn [2], is suggested that will assist life prediction techniques for situations of combined axial and torsional loading. Figure 15 shows low-cycle fatigue curves for AISI 316 stainless steel at 400°C for four different strain states. The upper curve is for pure torsion the lower

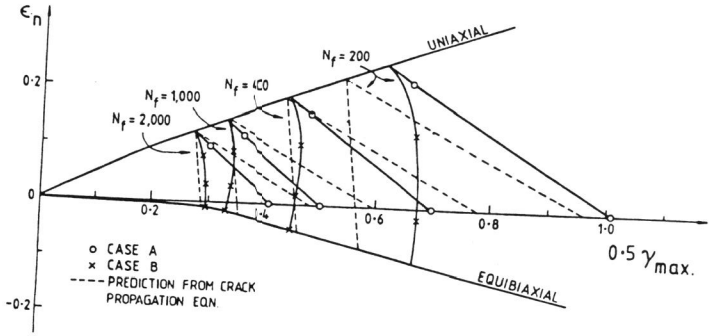

Fig. 14 Comparison of endurance data from experimental high strain fatigue tests and crack propagation predictions

curve for push-pull tests, representing Case A and Case B type cracking systems respectively. It is obvious that the octahedral shear strain, γ_{oct}, does not correlate these data. However by defining an equivalent shear strain $\Delta\bar{\gamma}$ by an equation of double parameter form i.e.

$$\Delta\bar{\gamma} = \Delta\gamma(1 + S(\epsilon_n/\gamma)^{\alpha})^{1/\alpha} \quad [7]$$

a single curve, Fig. 16, can correlate all the data of Fig. 15 when $\alpha = 2$ and $S = 60.8$. This single curve is represented by

$$\Delta\bar{\gamma}.N_f^{0.45} = 0.46 \quad [8]$$

It should be noted that the constants S and α are temperature dependent (21).

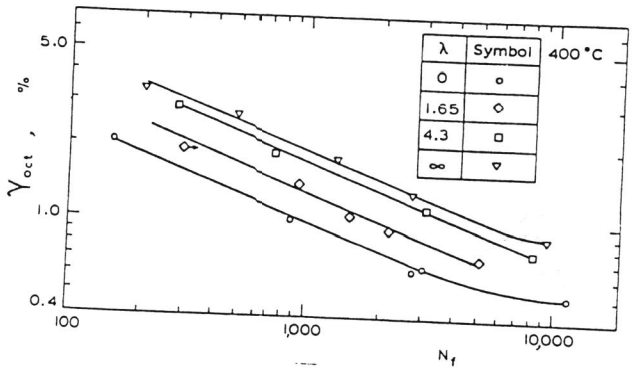

Fig. 15 Endurance curves as a function of octahedral shear strain for four strain states: AISI 316 stainless steel

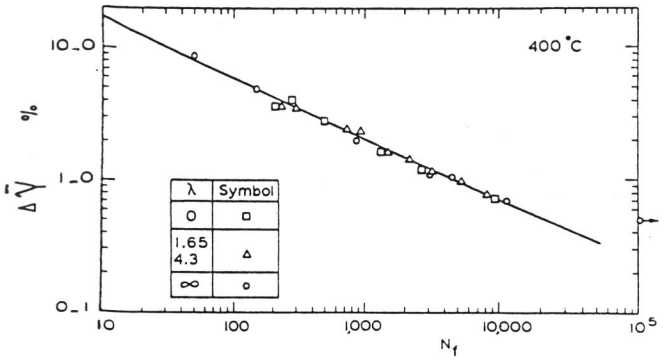

Fig. 16 An equivalent plastic shear strain range correlation for the data in Fig. 15

OUT-OF-PHASE LOADING

Out-of-phase loading conditions can produce several unusual effects, as already indicated, which assist our understanding of the fatigue process, both in terms of deformation behaviour, see Fig. 8, and fracture behaviour, see Fig. 11. When ϵ_1, ϵ_2 and ϵ_3 rotate during a cycle an infinite number of cracking systems can be operative throughout every cycle, and endurance is reduced because of the large values of ϵ_n that can be obtained. However a secondary effect is that lifetime can be extended due to crack growth on one plane being obstructed by other cracks on other planes. Similarly deformation behaviour is more complex due to the rotation of planes suffering maximum shear strain.

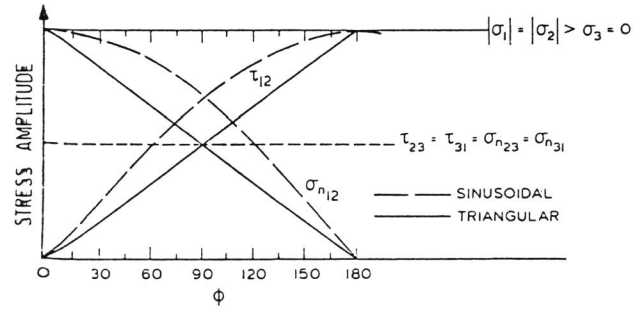

Fig. 17 Maximum stress levels on shear planes as a function of the out-of-phase angle between applied biaxial principal stresses σ_1 and σ_2

Even for the relatively simple biaxial stress system, shown in Fig. 12, for which σ_1 and σ_2 are equal ($\sigma_3 = 0$) and are applied out-of-phase by an angle ϕ, it has been shown (22) that three distinct cracking systems can operate within a single cycle, each one forming different crack growth planes.

Figure 17 shows the results of the stress analysis and indicates that when the phase angle is less than 90 degrees for triangular loading (or 60 degrees for sinusoidal loading) shear stresses $\tau_{23} = \tau_{31} > \tau_{12}$, and so the first two mentioned mutually perpendicular slip systems operate; each with the same value in magnitude of their respective normal stress, i.e. $\sigma_{n23} = \sigma_{n31}$. At 90 degrees (or 60 degrees, sinusoidal loading) all three systems are of equal magnitude, although they operate at different instants in the cycle, and so all three crack systems have an equal opportunity to become operative, consequently crack growth interference and fatigue life will be maximized, see Fig. 18. When $\phi > 90$ degrees only one crack system dominates, τ_{12}, and as ϕ increases further, lifetime will reduce due to a decreasing interference from the other two systems (22).

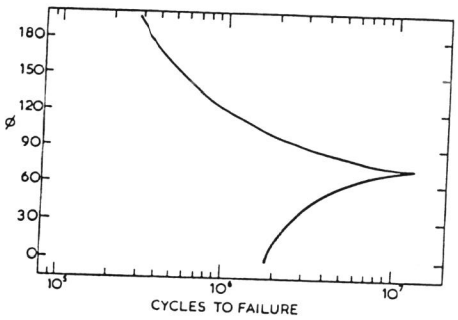

Fig. 18 The effect of phase angle on endurance.

CRACK GROWTH AND MIXED-MODE LOADING

As indicated in Fig. 3a, co-planar crack growth can occur theoretically by three separate modes, but depending on the spatial orientation and magnitude of the applied loads it is conceivable that the plane of crack growth can change so that one mode becomes dominant. Expressed another way stage I and stage II crack growth phases, since they have specific orientations to the 3-D strain state (which is a function of the loading system), may interchange depending on changes in loading pattern, residual stresses and geometrical factors. Of prime importance in these considerations are the threshold condition for crack growth under mixed-mode loading, the conditions for re-orientation of the crack growth plane, and branch crack instability.

Figure 19 shows the form of crack tip plasticity for cracks inclined at different angles in a uniaxially loaded plate (23). These angled cracks clearly are subjected to mixed-mode loading (mode I and mode II) and any re-orientation the crack may take will depend upon the degree of stress biaxiality of the external loading system and the initial crack angle. Once the crack changes direction the ratio of mixed mode loading is altered, as is the stress intensity value for such a branched crack (23).

Theoretical (24) and experimental (25) studies have been conducted to examine the fracture behaviour and the threshold behaviour of cracks subjected to mixed-mode loading. The elastic-plastic numerical analyses for

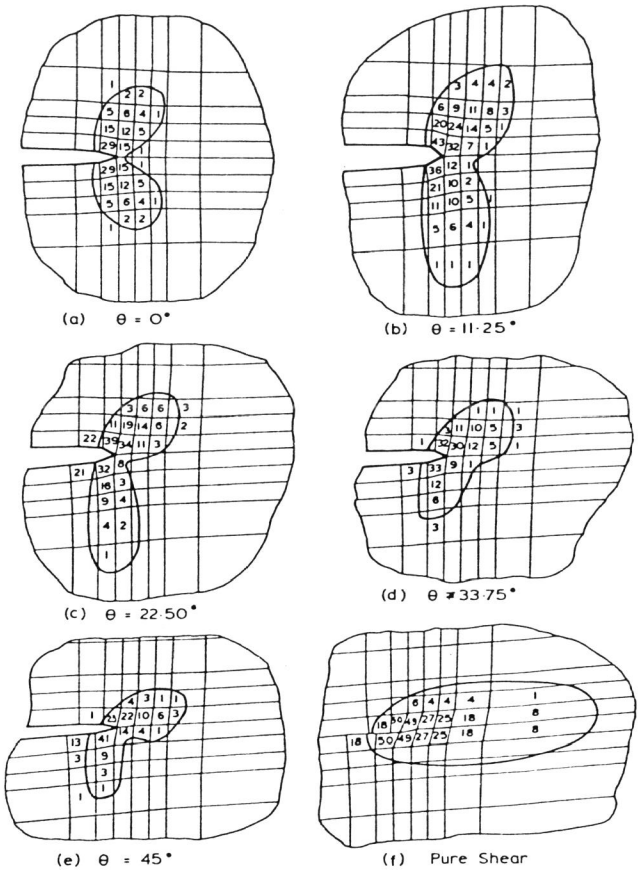

Fig. 19 Plastic zones for (a-e) different crack inclinations in a uniaxially loaded plate and (f) a pure shear loaded crack. The numbers in the elements are the average plastic equivalent strains x 10^4

crack instability conditions showed that LEFM theories could not explain previously conducted fracture experiments, and that the best fit to the data was the maximum tensile stress criterion while a safe lower bound solution was given by the G^{Δ} theory (strain energy release criterion for elastic-plastic materials) for a centre cracked panel (24).

Threshold studies in specimens of the form of Fig. 5c (25) showed that the creation of a branch crack is controlled not only by the mode I displacement but also the mode II component. The mode II component increases the size of the crack tip reversed plastic zone so facilitating fatigue crack growth. Thus the threshold for mode II takes a lower value than for mode I, see Fig. 20. However pure mode II, especially for long cracks, enhances contact and rubbing of crack surfaces as shear-mode growth occurs thereby causing

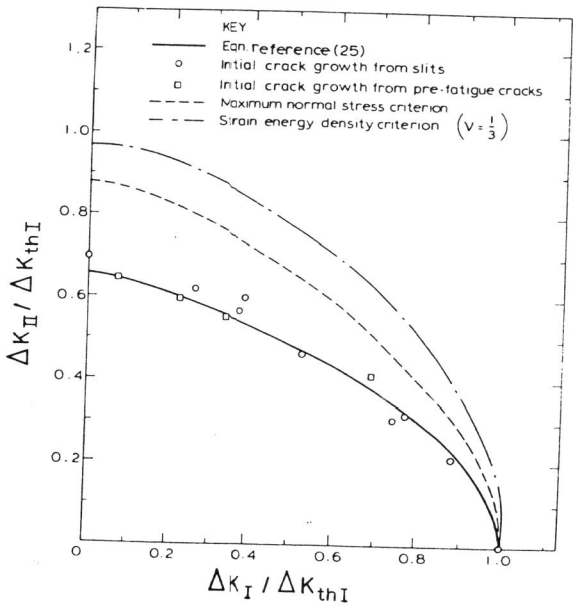

Fig. 20 Mixed-mode, LEFM crack growth thresholds: a comparison of theoretical predictions with experimental results

crack retardation and an eventual change to mode I growth.

A theoretical model for predicting the lower bound curve of Fig. 20 was proposed that showed very good agreement with experimental results and which gave a safe prediction for design purposes.

CUMULATIVE DAMAGE

The mose widely used hypothesis for assessing the accumulation of damage in variable stress range fatigue tests is that due to Palmgren (26) and Miner (27), namely

$$\sum n_i/N_{fi} = D \qquad [9]$$

Here n_i is the number of cycles applied at a constant stress or strain range level that corresponds to an endurance N_{fi}. Failure is assumed to occur when the summation of damage, D, reaches unity.

Equation [9] is a consequence of the propagation behaviour of a fatigue crack, which may be expressed as,

$$\frac{da}{dN} = A.\Delta\gamma_p^m a. \qquad [10]$$

since this may be integrated over the appropriate number of cycles n_i during which the cyclic plastic strain range, $\Delta\gamma_{pi}$, advances the crack; see (28). However at low load levels, the early growth of cracks (usually designated as crack "initiation") occupies a significant proportion of fatigue lifetime before the continuum mechanics expression, equation [10], can be used to model crack propagation. If fatigue damage is identified with crack length, as suggested previously, then for a loading sequence of high stress range followed by low, D must be less than unity because at high strain range the extensive period of "initiation" is evaded (29). Conversely, the reverse loading sequence gives values of D greater than unity.

However in multiaxial cumulative damage studies additional complications arise due to two other variable parameters namely the biaxial stress state and the phase angle. Should the phase angle or the principal stress axes change in a biaxial stress test, the following mutations can be postulated.

(a) Crack Rotation

The direction of the crack changes although the crack growth mode may still be the same.

(b) Reinitiation

When the previous plane of growth is unfavourable for the second phase of loading, then a new crack system requires to be initiated.

(c) Change of Mode

Stages and modes of crack growth change to accommodate the new stress-strain state.

(d) Crack interference

Crack growth is slowed down by transverse cracks created by the previous loading system.

(e) Stable growth

Crack propagation continues along the same initial path if the crack tip stress field is not too dissimilar to the initial loading system despite changes in the far stress field.

Should the equivalent stress or strain field remain unchanged but is reoriented with respect to the crack, this will minimise if not eliminate the sequence effects of initiation and propagation mentioned above. In such simplified multiaxial cumulative-damage tests, mutations (a)(c) and (e) should show damage summations D close to unity, but mutations (b) and (d) may considerably extend life, i.e. give values D > 1. Experimental results for tests in which the equivalent strain state is not changed (30) are shown in Fig. 21. Here the sense of twist was reversed after n_1 cycles in combined torsion-tension tests thereby rotating the principal axes of strain. Obviously by keeping the stress biaxiality λ ($=\Delta\gamma/\Delta\varepsilon$) constant, where $\Delta\gamma$ and $\Delta\varepsilon$ are the torsional and axial strain ranges respectively, N_{f1} and N_{f2} are identical. Figure 21(a) presents results for tests in which the principal stress axes were rotated by 45 degrees and hence the initial stage II crack growth plane became a stage I crack growth plane. Likewise one initial stage I crack growth plane became a stage II plane in the second phase of the cumulative damage test. For all of these tests

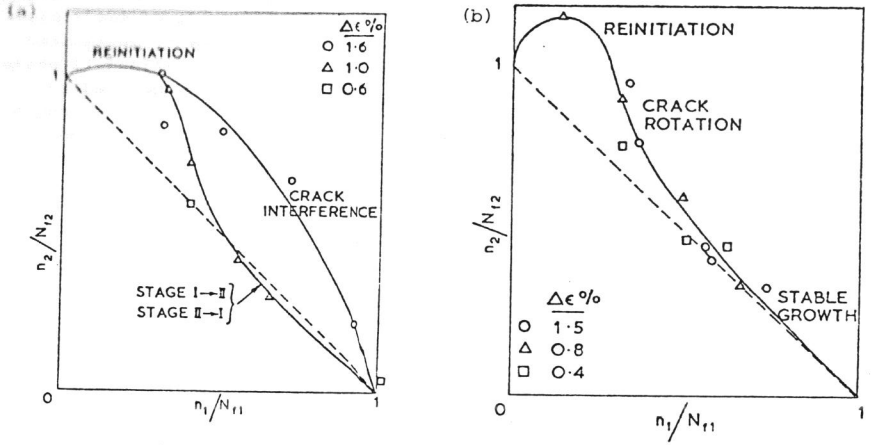

Fig. 21 Multiaxial cumulative damage test results
(a) λ = 1.5; principal axis rotation 45°
(b) λ = 4; principal axis rotation 21°

crack growth directions were observed using a X40 toolmakers microscope and of the hundreds of cracks measured most could be categorised as of either the stage I or stage II type. Cracks that initiated at polishing marks were excluded from the analysis.

For low values of n_1/N_{f1} it was necessary to reinitiate new cracks in the second phase because the initial small cracks were not dominant and presumably became non-propagating; therefore n_2/N_{f2} is unity. For higher values of n_1/N_{f1} and hence longer initial cracks the value of D is unity since stage I and stage II cracks simply changed to stage II and stage I cracks respectively. At high equivalent strain levels however there should be many more stage I cracks on the complementary shear plane, and these caused mutation (d), i.e. interference to crack growth during the second phase of the test since these cracks were unfavourably oriented.

In Fig. 21(b) the strain state of λ = 4 gave a rotation of principal strain axes of only 21 degrees which did not favour the interchangeability of stage I and stage II cracks. Rather the initial stage I cracks preferred either to rotate to the closest new shear plane following a phase change, mutation (a), or for longer initial cracks, i.e. higher initial fractions of n_1/N_{f1}, to remain on the original crack growth plane and continue to grow in a stable manner, mutation (e). In these tests no stage II cracks were observed, primarily because of the relatively high value of the shear strain range $\Delta\gamma$. As in previous tests it is also noted that re-initiation was necessary in the second phase for low initial values of n_1/N_{f1}.

ANISOTROPIC BEHAVIOUR

All materials subjected to cyclic loading develop anisotropic behaviour. As shown on pages 7 and 8 the cyclic deformation response is best related to the specific planes of maximum shear stress and strain. Distortions to hysteresis loops occur should out-of-phase loading be introduced because

the planes of maximum shear will rotate and therefore intersect with previous slip planes causing additional anisotropic cyclic hardening. Even before plastically cycling a material it may exhibit a marked texture, e.g. alternate bands of ferrite and pearlite as in rolled plain carbon steels. A consequence of this is that fatigue cracks may not follow similar paths, growth rates and shapes compared to those in pure metals. Finally it may be noted that any incompatability of fatigue data generated from tests on the same material but on specimens of different shape, size and orientation is frequently cited as being caused by anisotropy. It is only by rigorous control of multiaxial fatigue testing conditions that all these effects can be studied independently (see the next section).

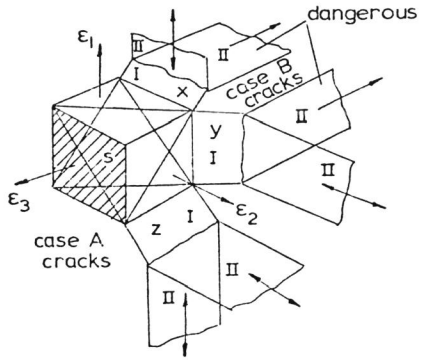

Fig. 22 Various crack growth planes and directions

Figure 22 shows how Case A and Case B cracks can be generated in relation to their specific three-dimensional stress-strain fields. Both types of crack can have their growth rates and hence lifetimes modified due to changes in crack tip plastic zone size, shape and orientation due to differences in yield stress, work hardening behaviour and fracture strain, i.e. non-isotropic behaviour. No systematic studies of these effects have been reported but certain changes in fracture behaviour can be discussed.

With reference to Fig. 22, the X-plane systems will operate when $|\varepsilon_1-\varepsilon_3| > |\varepsilon_1-\varepsilon_2|$ and $|\varepsilon_2-\varepsilon_3|$. However if ε_2 approaches the value of ε_1 and the Y system is relatively weak in a fracture sense, the crack orientation will change to the Y system. It should be noted that in push-pull tests $\varepsilon_2 = \varepsilon_3$ and both X and Z stage I cracks can form simultaneously; see also Fig. 9.

When the orientation of ε_1, ε_2 and ε_3 changes such that ε_2 is perpendicular to the surface, then Case A cracking on one of the complementary Z systems is the norm but, as is often appreciated in torsion tests, cracks will either prefer to grow along the specimen axis direction or circumferentially depending on textural anisotropy. Case B cracking on the X (or Y) system is only possible when ε_2 is almost equal to ε_3 (or ε_1) i.e. uniaxial tension (or compression), or the material is anisotropic.

A UNIVERSAL MULTIAXIAL FATIGUE FACILITY

From the foregoing discussions it is clear that in biaxial-multiaxial fatigue studies material anisotropy, specimen shape and loading conditions all have serious consequences on fatigue results. In an endeavour to eliminate as many variables as possible it was decided to construct a universal multiaxial test facility at Sheffield, with the aid of a generous grant from the SERC, that could cover a wide range of stress levels and all biaxial stress states. Accordingly a tubular specimen was selected that could be tested both in low stress and high strain fatigue.

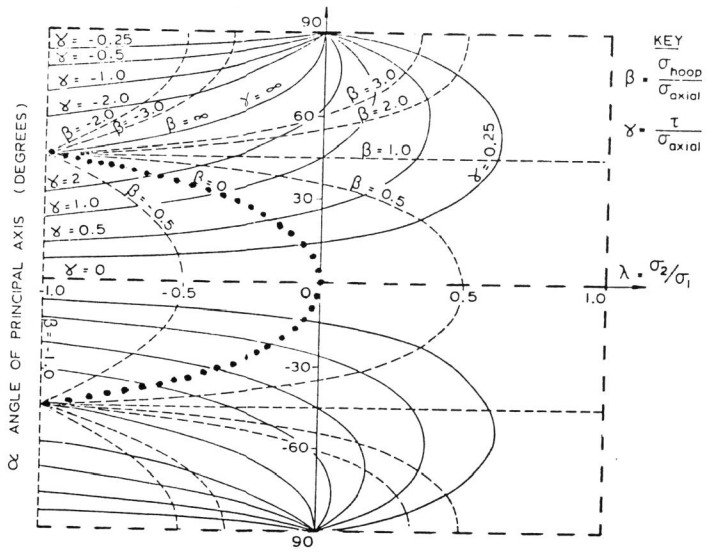

Fig. 23 Contours of all various stress states that can be induced in a single specimen by the new machine

More important however is that all strain states can be achieved, see Fig. 23. Previous biaxial-multiaxial fatigue machines could only follow the conditions shown dotted (torsion + axial loading) or heavy dashed (axial + int/ext. pressurization). By a judicious selection of β (ratio of tensile hoop stress and axial stress) and γ (ratio of the torsion shear stress and axial stress) any biaxial stress loading can be achieved by subjecting the tubular specimen to various but precise combinations of reversed torsion, push-pull and internal/external pressure loads. Furthermore any biaxial stress ratio can be achieved with a selected orientation to the specimen axis so that a chosen crack system can be generated on any required plane thereby permitting a detailed study of the effects of anisotropy. In Fig. 23 the value of α is the angle between the maximum principal stress and the specimen axis. Since the loading systems are independently controlled by a microprocessor, complex out-of-phase studies can also be attempted. This machine is now being commissioned and experiments are soon to begin.

CONCLUSIONS

1. Fatigue fracture is governed by two parameters which describe the stress-strain space to which a material is subjected; no known single parameter is sufficient. In axial loading tests the second variable is proportional to the first variable and so push-pull data can not be universally representative of other test conditions.

2. Two types of cracking are identified, Case A cracks which are generated in the surface of a material, as in torsion loading, and Case B cracks which propagate into the interior of the body, as in plane strain and equibiaxial loading.

3. The type of crack system (Case A or Case B) is related to the orientation of the minimum principal strain with respect to the surface plane. For Case B it is normal to the surface, for Case A it is parallel to the surface.

4. Von Mises theory is not applicable to fatigue fracture and the Tresca theory is a more appropriate criterion to describe multiaxial cyclic deformation behaviour.

5. In biaxial-multiaxial fatigue research it is essential to relate the three-dimensional cyclic stress-strain state to the characteristics of crack growth, as well as to note any material anisotropy; also great care should be taken in the designing of specimens.

REFERENCES

1. Forsyth, P.J.E. (1961) Proc. Crack Propagation Symp. Cranfield, U.K., 76-94.
2. Brown, M.W. and Miller, K.J. (1973) Proc. Instn. Mech. Eng., 187 745-755 and D229-D244.
3. Brown, M.W. (1978) J. Strain Analysis, 13, 23-28.
4. Basquin, O.H. (1910) Proc. Am. Soc. Testing and Materials, 10, 625-630.
5. Coffin, L.F. (1954) Trans. Am. Soc. Mech. Engrs., 76, 931-950.
6. Manson, S.S. (1954) Nat. Advis. Comm. Aeronautics, Tech. Note 2933.
7. Paris, P.C. and Erdogan, F. (1963) Trans. Am. Soc. Mech. Engrs. (Series D) 85, 528-534.
8. Parsons, M.W. and Pascoe, K.J. (1974) Proc. Instn. Mech. Engrs. 188, 657-671.
9. Kanazawa, K., Miller, K.J. and Brown, M.W. (1979) J. Fatigue Eng. Materials and Structures, 2, 217-228.
10. Brown, M.W. and Miller, K.J. (1979) J. Fatigue Eng. Materials and Structures, 1, 93-106.
11. Brown, M.W. and Miller, K.J. (1979) J. Fatigue Eng. Materials and Structures, 1, 231-246.
12. Kanazawa, K., Miller, K.J. and Brown, M.W. (1977) J. Eng. Materials and Technology. ASME, 99H, 222-228.
13. Miller, K.J. and Kfouri, A.P. (1974) Int. J. Fracture, 10, 393-404.
14. Miller, K.J. (1977) Metal Science Journal, 11, 432-438.
15. Kibler, J.J. and Roberts, R. (1970) J. Eng. Ind. A.S.M.E., 92B, 727-734.
16. Zamrik, S.Y. and Shabara, M.A. (1975) Proc. Fourth Inter-American Conference on Materials Technology, 472-477.
17. Leevers, P.S., Culver, L.E. and Radon, J.C. (1979) Eng. Frac. Mech., 487-498.

18. Charvat, I.M.H. and Garrett, G.G. (1980) J. Test. Eval., 8, 9-17.
19. Adams, N.J.I. (1973) Proc. ICF 3 (Munich) paper 522/A.
20. Ellison E.G. and Andrews, J.M.H. (1973) J. Strain Analysis, 8, 209-219.
21. Kandil, F.A., Brown, M.W. and Miller, K.J. (1981) Proc. Int. Conf. Mech. Behaviour and Nuclear Applications of Stainless Steel at Elevated Temperatures, Metals Soc., 203-209.
22. Miller, K.J. (1976) Fatigue Testing and Design; Soc. Environ. Engs. 1, 13/1-13/17.
23. Kfouri, A.P. and Miller, K.J. (1981) Three Dimensional Constitutive Relations and Ductile Fracture North Holland Pub. Co., 83-109.
24. Wang, T.C. and Miller, K.J. (1984) Eng. Fract. Mech., 19, 621-632.
25. Gao, H., Brown, M.W. and Miller, K.J. (1982) Fat. Eng. Materials and Structures, 5, 1-17.
26. Palmgren, A.Z. (1924) Z. Ver. dt. Ing., 68, 339-341.
27. Miner, M.A. (1945) J. App. Mech., 12, A159-164.
28. Miller, K.J. and Gardiner, T. (1977) J. Strain Analysis, 12, 253-261.
29. Miller, K.J. and Ibrahim, M.F.E. (1981) J. Fatigue Eng. Materials and Structures, 4, 263-277.
30. Brown, M. W., Miller, K.J. and Liu, H. W. (1983) Proc. ICF Symp. Fracture Mechanics, Science Press, Beijing, 629-634.

BIBLIOGRAPHY

ASTM (1984) Special Technical Publication, Biaxial/Multiaxial Fatigue, STP 853 Eds. Miller, K.J. and Brown, M.W. To be published 1984.
Brown, M.W. and Miller, K.J. (1979) J. Fatigue Eng. Materials and Structures, 1, 217-229.
Brown, M. W. and Miller, K.J. (1980) Int. Symp. on Defects and Fracture, Tuczno, Poland. Pub: Martinus Nijhoff (1980), 29-38.
Brown, M.W. and Miller, K.J. (1981) J. Testing and Evaluation (ASTM) 202-208
Brown, M.W. and Miller, K.J. (1982) ASTM STP 770, 482-499.
Brown, M.W., Miller, K.J. and Walker, T.J. (1983) Proc. VIII SMIRT Conference L, 143-149.
Gao H., de los Rios, E.R. and Miller, K.J. (1983) J. Fatigue Eng. Materials and Structures, 6, 137-148.
Gao, H., Brown, M.W. and Miller, K.J. (1983) Proc. ICF Symp. on Fracture Mechanics, Science Press, Beijing, 666-671.
Hopper, C.D. and Miller, K.J. (1977) J. Strain Analysis, 12, 23-28.
Kfouri, A.P. and Miller, K.J. (1979) ASTM STP 668, 214-228.
Kfouri, A.P. (1983) Proc. ICF Symp. on Fracture Mechanics, Science Press, Beijing, 76-81.
Liddle, M. and Miller, K.J. (1973) Proc. ICF (Munich), paper V-523A.

ACKNOWLEDGEMENTS

The authors would thank the following organizations who for many years have supported work on biaxial-multiaxial fatigue: The Science and Engineering Research Council, The United Kingdom Atomic Energy Authority, The Central Electricity Generating Board, and the United States Nuclear Regulatory Commission. Likewise the authors are indebted for contributions made by research students and overseas visitors together with resident staff at Sheffield.